

Ce_{1-x}Cu_xO_{2-x}/Al₂O₃/FeCrAl catalysts for catalytic combustion of methane

Fengxiang Yin, Shengfu Ji*, Nengzhan Chen, Meili Zhang, Liping Zhao, Chengyue Li*, Hui Liu

The Key Laboratory of Science and Technology of Controllable Chemical Reactions, Ministry of Education, Beijing University of Chemical Technology, 15 Beisanhuan Dong Road, P.O. Box 35, Beijing 100029, China

Available online 11 July 2005

Abstract

A series of the Ce_{1-x}Cu_xO_{2-x}/Al₂O₃/FeCrAl catalysts ($x = 0-1$) were prepared. The structure of the catalysts was characterized using XRD, SEM and H₂-TPR. The catalytic activity of the catalysts for the combustion of methane was evaluated. The results indicated that in the Ce_{1-x}Cu_xO_{2-x}/Al₂O₃/FeCrAl catalysts the surface phase structure were the Ce_{1-x}Cu_xO_{2-x} solid solution, α -Al₂O₃ and γ -Al₂O₃. The surface particle shape and size were different with the variety of the molar ratio of Ce to Cu in the Ce_{1-x}Cu_xO_{2-x} solid solution. The Cu component of the Ce_{1-x}Cu_xO_{2-x}/Al₂O₃/FeCrAl catalysts played an important role to the catalytic activity for the methane combustion. There were the stronger interaction among the Ce_{1-x}Cu_xO_{2-x} solid solution and the Al₂O₃ washcoats and the FeCrAl support.

© 2005 Elsevier B.V. All rights reserved.

Keywords: Monolithic catalysts; Washcoat; Methane catalytic combustion; Ce_{1-x}Cu_xO_{2-x} solid solution; XRD; SEM; TPR

1. Introduction

The catalytic combustion of the methane and volatile organic compounds represents a family of new technology in improvements of energy efficiency and air pollution prevention. Nowadays, most of the combustion catalysts are supported noble metal catalysts, or transition metal oxide catalysts [1–2]. Recently, the structured monolithic catalysts and reactors, especially that of use the metal as the catalyst supports, have gained considerable attention due to greatly reduced pressure drops and more favorable heat transfer properties compared to conventional packed-bed reactors loaded with catalyst pellets [3–5]. Kucharczky and co-workers found that in the monolithic Pd-based catalysts on heat-resisting FeCrAl alloy foil support palladium was deposited either onto pure aluminium oxide (Pd/Al₂O₃) or onto Al₂O₃ modified with SiO₂ (Pd/Al₂O₃-SiO₂) or with ZrSiO₄ (Pd/Al₂O₃-ZrSiO₄) and that the Al₂O₃ and the

modification of Al₂O₃ washcoats were important for the active form of the palladium [6]. Artizzu et al. found that copper oxide deposited onto high surface area magnesium aluminate spinel with the cordierite as the support is very active for methane combustion at high GHSV [7]. Liu and Flytzani-Stephanopoulos found that the Cu–Ce–O system was one of the most active catalyst systems for the total oxidation [8]. The aim of this study is to examine the activity of Ce_{1-x}Cu_xO_{2-x} ($x = 0-1$) solid solution based FeCrAl alloy foils monolithic catalysts with Al₂O₃ washcoats for the methane catalytic combustion and to understand the structure of the Ce_{1-x}Cu_xO_{2-x}/Al₂O₃/FeCrAl catalysts.

2. Experimental

2.1. Catalysts preparation

The monolithic catalysts were prepared using the FeCrAl alloy foils (OC404, Sandvik Steel, Sweden) as supports. A three-step procedure was used to deposit Al₂O₃ layers and

* Corresponding authors. Tel.: +86 10 64412054; fax: +86 10 64419619.
E-mail addresses: jisf@mail.buct.edu.cn (S. Ji), licy@mail.buct.edu.cn (C. Li).

metal oxide solid solution layers: (1) the foils were cleaned in ethanol, acidic, and basic solution, and then, were calcined at 950 °C for 15 h; (2) a boehmite primer sol was used as first washcoat layers to improve the adhesion between the metal oxide solid solution layers and the oxidized metallic support; (3) the mixture slurry of the $\text{Ce}_{1-x}\text{Cu}_x\text{O}_{2-x}$ ($x = 0-1$) solid solution, which were prepared using the urea-nitrate combustion method [9], and $\gamma\text{-Al}_2\text{O}_3$ was deposited on the first washcoat layers. Finally, the $\text{Ce}_{1-x}\text{Cu}_x\text{O}_{2-x}/\text{Al}_2\text{O}_3/\text{FeCrAl}$ metal support structured catalysts were prepared. The weight of metal oxide solid solution layers and Al_2O_3 layers are ca. 5 wt.% and ca. 10 wt.%, respectively.

2.2. Catalysts characterization

The surface phase structure of the coatings was measured by X-ray powder diffraction (XRD) using a Rigaku D/Max 2500 VB2+/PC diffractometer with Cu K α radiation. The morphology of the samples was observed by Cambridge Instruments Streoscan 250 MK3 scanning electron microscope (SEM). Temperature programmed reduction (TPR) experiments were performed using a Thermo Electron Corporation TPD/R/O 1100 Series Catalytic Surfaces Analyzer equipped with a TCD detector. The coating adhesion was measured by an ultrasonic method. The weight loss of the washcoat layers was less than 2 wt.%.

2.3. Catalytic activity measurements

The catalytic activity was measured using a conventional quartz flow reactor (i.d., 6 mm; length, 300 mm) at atmospheric pressure. The test was performed with cylindrical monolithic catalysts, which are made up of several cylinders in different diameter and 50 mm in length. Methane combustion involved a gas mixture of 2 vol.% of CH_4 in air, with a gas hourly space velocity (GHSV) of 5200; 10,400 and 20,800 ml/g (cat + Al_2O_3) h. The reaction of methane combustion was stabilized for 20 min, and the outlet products were measured with gas chromatography (Beijing East & West Electronics Institute, GC-4000A). In every case, carbon dioxide and water were the only reaction products detected along the whole experiment.

3. Results and discussion

3.1. Fresh catalysts characterization

Fig. 1 shows the XRD patterns of FeCrAl metallic support and $\text{Ce}_{1-x}\text{Cu}_x\text{O}_{2-x}/\text{Al}_2\text{O}_3/\text{FeCrAl}$ monolithic catalysts. It can be seen that the characteristic peaks of FeCr (2θ is 44.3° and 64.6°, JCPDS 34-0396) and $\alpha\text{-Al}_2\text{O}_3$ (2θ is 25.5°, 35.0°, 37.6°, 43.2°, 52.4°, 57.3°, 66.3° and 68.0°, respectively (JCPDS 88-0826, Fig. 1A). It is indicated that, after the heat treatment, $\alpha\text{-Al}_2\text{O}_3$ is formed on the FeCrAl

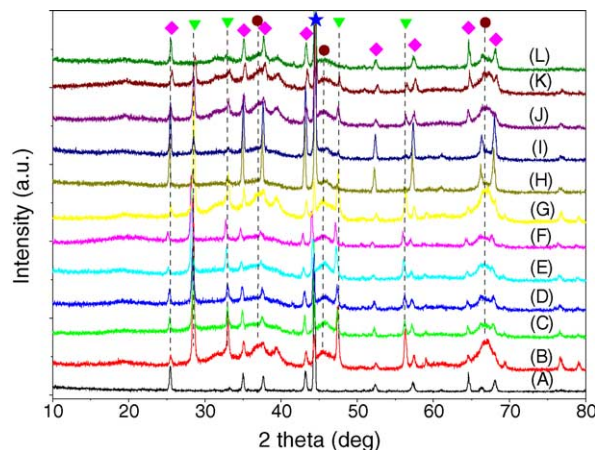


Fig. 1. XRD patterns of the metallic support pre-oxidized and the fresh monolithic catalysts: (A) FeCrAl foil pre-oxidized at 950 °C for 15 h; (B) $\text{CeO}_2/\text{Al}_2\text{O}_3/\text{FeCrAl}$; (C) $\text{Ce}_{0.9}\text{Cu}_{0.1}\text{O}_{1.9}/\text{Al}_2\text{O}_3/\text{FeCrAl}$; (D) $\text{Ce}_{0.8}\text{Cu}_{0.2}\text{O}_{1.8}/\text{Al}_2\text{O}_3/\text{FeCrAl}$; (E) $\text{Ce}_{0.7}\text{Cu}_{0.3}\text{O}_{1.7}/\text{Al}_2\text{O}_3/\text{FeCrAl}$; (F) $\text{Ce}_{0.6}\text{Cu}_{0.4}\text{O}_{1.6}/\text{Al}_2\text{O}_3/\text{FeCrAl}$; (G) $\text{Ce}_{0.5}\text{Cu}_{0.5}\text{O}_{1.5}/\text{Al}_2\text{O}_3/\text{FeCrAl}$; (H) $\text{Ce}_{0.4}\text{Cu}_{0.6}\text{O}_{1.4}/\text{Al}_2\text{O}_3/\text{FeCrAl}$; (I) $\text{Ce}_{0.3}\text{Cu}_{0.7}\text{O}_{1.3}/\text{Al}_2\text{O}_3/\text{FeCrAl}$; (J) $\text{Ce}_{0.2}\text{Cu}_{0.8}\text{O}_{1.2}/\text{Al}_2\text{O}_3/\text{FeCrAl}$; (K) $\text{Ce}_{0.1}\text{Cu}_{0.9}\text{O}_{1.1}/\text{Al}_2\text{O}_3/\text{FeCrAl}$; (L) $\text{CuO}/\text{Al}_2\text{O}_3/\text{FeCrAl}$ catalysts: (★) FeCr; (▼) $\text{Ce}_{1-x}\text{Cu}_x\text{O}_{2-x}$ solid solution; (●) $\gamma\text{-Al}_2\text{O}_3$; (◆) $\alpha\text{-Al}_2\text{O}_3$.

surface due to the segregation and oxidation of aluminium. The characteristic peaks of $\text{Ce}_{1-x}\text{Cu}_x\text{O}_{2-x}$ solid solution in the catalysts can be seen at 28.7°, 33.1°, 47.6° and 56.5°, respectively. However, the intensity of the peaks of $\text{Ce}_{1-x}\text{Cu}_x\text{O}_{2-x}$ is different with the molar ratio of Ce to Cu. In practically, no peaks of CuO, which, in general, are the most intensity peaks at 35.5 and 38.8 (JCPDS 45-0937), is detected in the $\text{CuO}/\text{Al}_2\text{O}_3/\text{FeCrAl}$ catalyst (Fig. 1L). Suggesting that the molar ratio of Ce to Cu influences strongly to the surface phase structure of the $\text{Ce}_{1-x}\text{Cu}_x\text{O}_{2-x}$ in the $\text{Ce}_{1-x}\text{Cu}_x\text{O}_{2-x}/\text{Al}_2\text{O}_3/\text{FeCrAl}$ catalyst.

The morphology of FeCrAl metallic support and $\text{Ce}_{1-x}\text{Cu}_x\text{O}_{2-x}/\text{Al}_2\text{O}_3/\text{FeCrAl}$ monolithic catalysts were shown in Fig. 2. It was found that the whiskers of the Al_2O_3 were formed when the FeCrAl metallic support was calcined at 950 °C for 15 h in air (Fig. 2A). It is similar to the literature [10,11]. For $\text{Ce}_{1-x}\text{Cu}_x\text{O}_{2-x}/\text{Al}_2\text{O}_3/\text{FeCrAl}$ catalysts, the particle shape and size of the $\text{Ce}_{1-x}\text{Cu}_x\text{O}_{2-x}$ are different with the molar ratio of Ce to Cu. When Ce component is higher or lower, the particle size is bigger (Fig. 2B–D, J–L). However, the molar ratio of Ce is 0.7–0.3, the particle size is smaller (Fig. 2E–I). Indicating that the dispersancy of the $\text{Ce}_{1-x}\text{Cu}_x\text{O}_{2-x}$ solid solution in $\gamma\text{-Al}_2\text{O}_3$ depends on the molar ratio of Ce to Cu of the $\text{Ce}_{1-x}\text{Cu}_x\text{O}_{2-x}$.

3.2. Activity of monolithic $\text{Ce}_{1-x}\text{Cu}_x\text{O}_{2-x}/\text{Al}_2\text{O}_3/\text{FeCrAl}$ catalysts

The catalytic activity for methane combustion was evaluated at temperature from 400 to 750 °C and the results were shown in Figs. 3–5. It was found that the catalytic activity of the catalysts depended strongly on the molar ratio of the Ce and Cu in the $\text{Ce}_{1-x}\text{Cu}_x\text{O}_{2-x}$ solid solution in

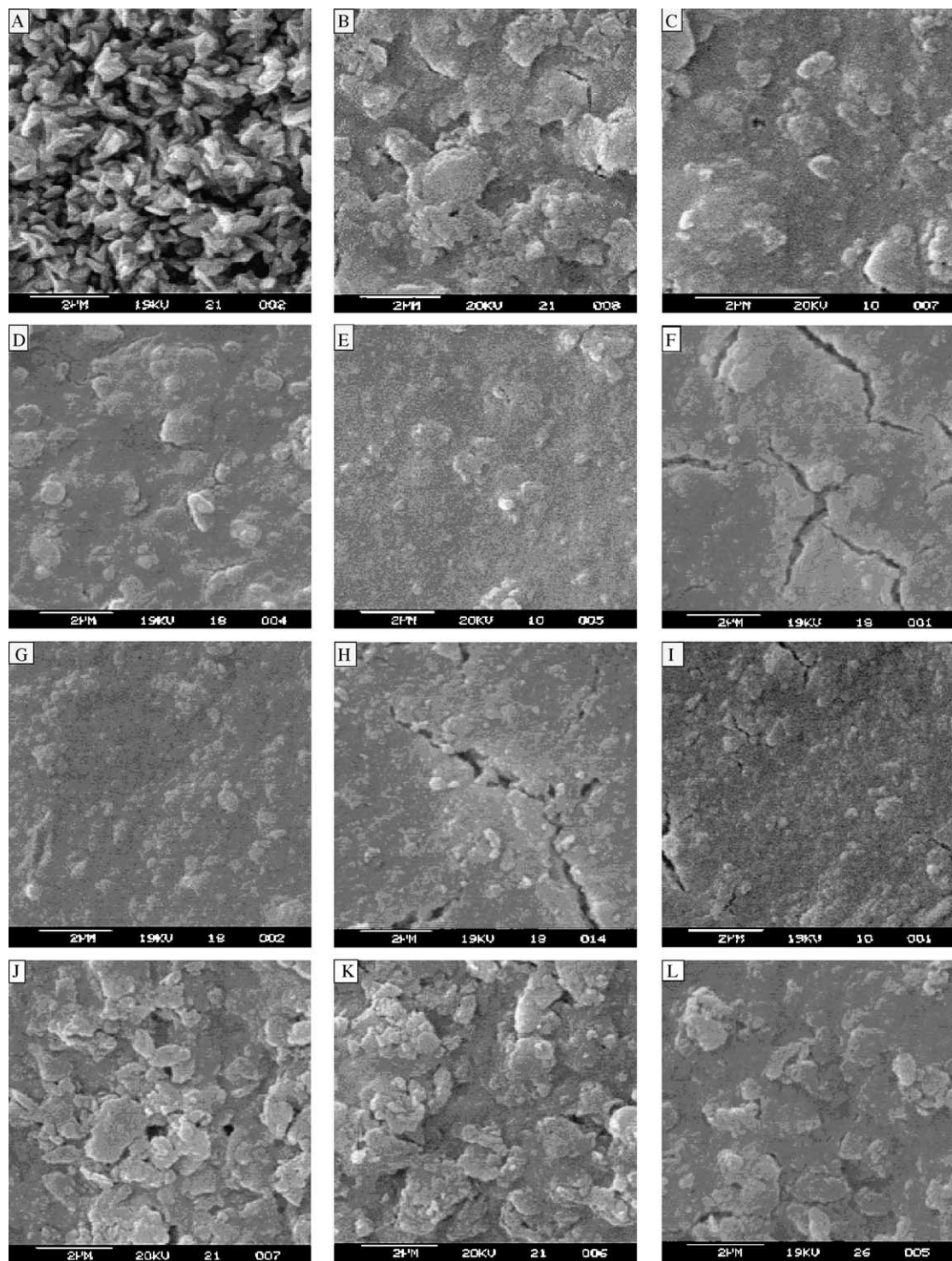


Fig. 2. SEM images of the metallic support pre-oxidized and the fresh monolithic catalysts: (A) FeCrAl foil pre-oxidized at 950 °C for 15 h; (B) CeO₂/Al₂O₃/FeCrAl; (C) Ce_{0.9}Cu_{0.1}O_{1.9}/Al₂O₃/FeCrAl; (D) Ce_{0.8}Cu_{0.2}O_{1.8}/Al₂O₃/FeCrAl; (E) Ce_{0.7}Cu_{0.3}O_{1.7}/Al₂O₃/FeCrAl; (F) Ce_{0.6}Cu_{0.4}O_{1.6}/Al₂O₃/FeCrAl; (G) Ce_{0.5}Cu_{0.5}O_{1.5}/Al₂O₃/FeCrAl; (H) Ce_{0.4}Cu_{0.6}O_{1.4}/Al₂O₃/FeCrAl; (I) Ce_{0.3}Cu_{0.7}O_{1.3}/Al₂O₃/FeCrAl; (J) Ce_{0.2}Cu_{0.8}O_{1.2}/Al₂O₃/FeCrAl; (K) Ce_{0.1}Cu_{0.9}O_{1.1}/Al₂O₃/FeCrAl; (L) CuO/Al₂O₃/FeCrAl catalysts.

selective GHSV and the reaction conditions. When the GHSV was 5200 ml/g (cat + Al₂O₃) h, the Ce_{1-x}Cu_xO_{2-x}/Al₂O₃/FeCrAl catalysts ($x = 0.8-0.6$) had the best catalytic activity. The temperature of methane combusted completely was at ca. 550 °C (Fig. 3). When the GHSV was increase, the

temperature of methane combusted completely became higher. For example, the GHSV was 10,400 ml/g (cat + Al₂O₃) h, the temperature of methane combusted completely was at ca. 600 °C for the Ce_{1-x}Cu_xO_{2-x}/Al₂O₃/FeCrAl catalysts ($x = 0.8-0.7$) (Fig. 4). The GHSV was 20,800 ml/g

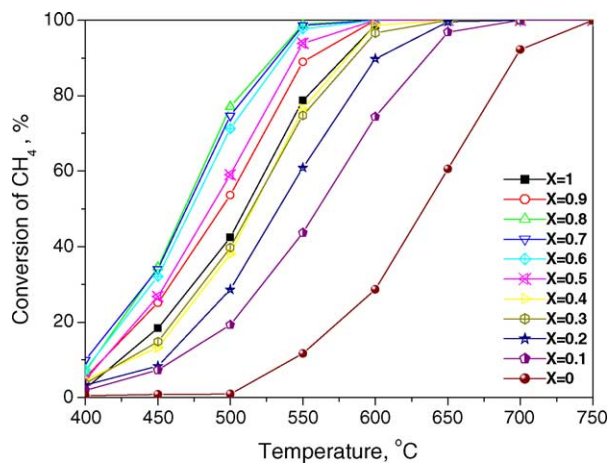


Fig. 3. Methane conversion over the $\text{Ce}_{1-x}\text{Cu}_x\text{O}_{2-x}/\text{Al}_2\text{O}_3/\text{FeCrAl}$ catalysts. GHSV = 5200 ml/g (cat + Al_2O_3) h.

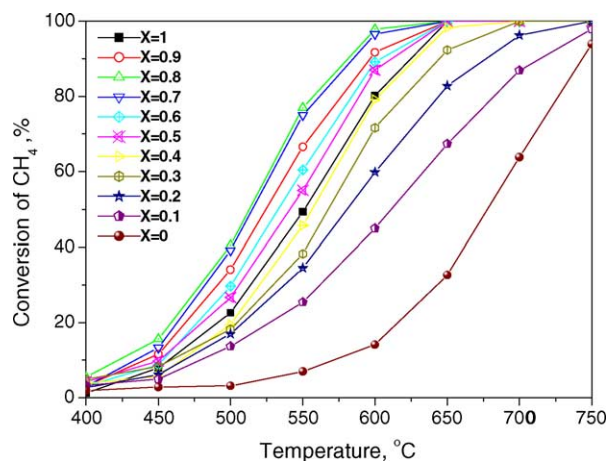


Fig. 4. Methane conversion over the $\text{Ce}_{1-x}\text{Cu}_x\text{O}_{2-x}/\text{Al}_2\text{O}_3/\text{FeCrAl}$ catalysts. GHSV = 10,400 ml/g (cat + Al_2O_3) h.

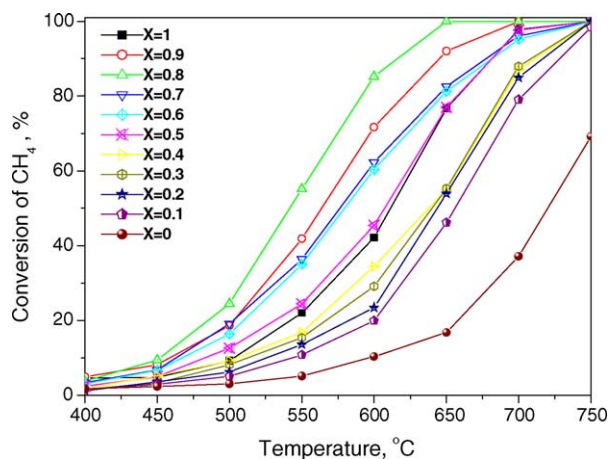


Fig. 5. Methane conversion over the $\text{Ce}_{1-x}\text{Cu}_x\text{O}_{2-x}/\text{Al}_2\text{O}_3/\text{FeCrAl}$ catalysts. GHSV = 20,800 ml/g (cat + Al_2O_3) h.

(cat + Al_2O_3) h, the temperature of methane combusted completely was at ca. 650 °C for the $\text{Ce}_{1-x}\text{Cu}_x\text{O}_{2-x}/\text{Al}_2\text{O}_3/\text{FeCrAl}$ catalysts ($x = 0.8$) (Fig. 5). However, the $\text{CeO}_2/\text{Al}_2\text{O}_3/\text{FeCrAl}$ catalyst had the lowest activity in all case. Suggesting that the molar ratio of the Ce and Cu in the $\text{Ce}_{1-x}\text{Cu}_x\text{O}_{2-x}/\text{Al}_2\text{O}_3/\text{FeCrAl}$ catalysts ($x = 0-1$) plays an important role to the catalytic activity of the catalysts for the methane combustion.

From Figs. 3–5, it is found that the catalyst of higher copper components have better catalytic performance under some conditions. It is indicated that the copper oxide species are more active than the ceria oxide species in the $\text{Ce}_{1-x}\text{Cu}_x\text{O}_{2-x}/\text{Al}_2\text{O}_3/\text{FeCrAl}$ catalysts. Gellings and Bouwmeester had given some important relationship between catalytic behaviour and solid state properties of the oxides catalysts and the oxygen flux may alter the relative presence of different oxygen species on the catalyst surface [12]. Hence, a suitable molar ratio of the Ce and Cu in the $\text{Ce}_{1-x}\text{Cu}_x\text{O}_{2-x}/\text{Al}_2\text{O}_3/\text{FeCrAl}$ catalysts may be advantageous for the copper oxide species.

3.3. H_2 -TPR measurements

TPR profiles of the $\text{Ce}_{1-x}\text{Cu}_x\text{O}_{2-x}/\text{Al}_2\text{O}_3/\text{FeCrAl}$ catalysts were presented in Fig. 6. It is found that there is the more difference with the molar ratio of the Ce and Cu in the catalysts. For the $\text{CuO}/\text{Al}_2\text{O}_3/\text{FeCrAl}$ catalyst, the peaks of reduction are observed at ca. 302, 501 and 705 °C and the peak at ca. 302 °C is the biggest. However, with increase of Ce component in the $\text{Ce}_{1-x}\text{Cu}_x\text{O}_{2-x}/\text{Al}_2\text{O}_3/\text{FeCrAl}$ catalysts, the peaks at 302 and 501 °C shift to the more higher temperature and the consumption of H_2 become the less. The peak at 705 °C shift to the lower temperature and the consumption of H_2 become obviously the larger. It is indicated that the Ce component in the catalysts can influence the temperature of reduction and the consumption of H_2 . From 300 to 600 °C, when the Ce component is lower,

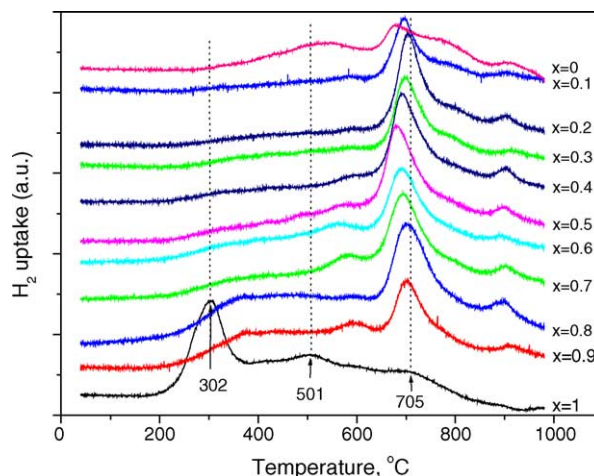


Fig. 6. TPR patterns of the $\text{Ce}_{1-x}\text{Cu}_x\text{O}_{2-x}/\text{Al}_2\text{O}_3/\text{FeCrAl}$ catalysts.

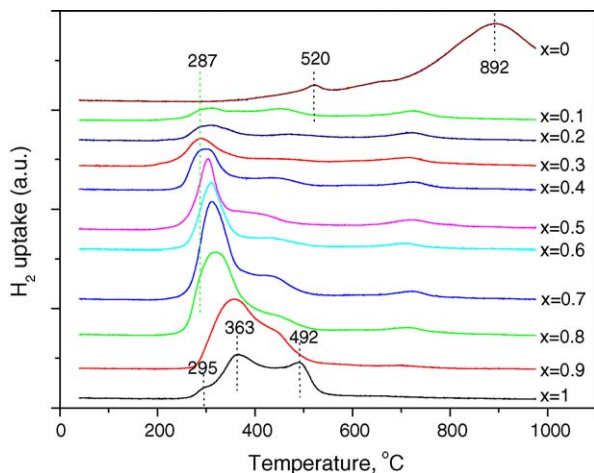


Fig. 7. TPR patterns of the $\text{Ce}_{1-x}\text{Cu}_x\text{O}_{2-x}$ solid solution.

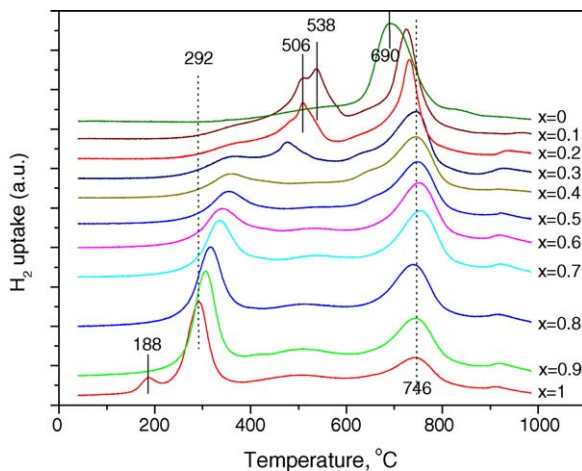


Fig. 8. TPR patterns of the $\text{Ce}_{1-x}\text{Cu}_x\text{O}_{2-x}/\text{Al}_2\text{O}_3$.

the consumption of H_2 is more. With the Ce component increased, the consumption of H_2 is less and less. Suggesting that the oxide species of the consumption of H_2 from 300 to 600 °C play an important role to the methane catalytic combustion.

For comparison, the H_2 -TPR of the pure $\text{Ce}_{1-x}\text{Cu}_x\text{O}_{2-x}$ and the $\text{Ce}_{1-x}\text{Cu}_x\text{O}_{2-x}/\text{Al}_2\text{O}_3$ were measured. The TPR profiles were shown in Figs. 7 and 8. It is found that both the temperature of reduction and the consumption of H_2 are obviously dissimilarity. In the pure $\text{Ce}_{1-x}\text{Cu}_x\text{O}_{2-x}$ samples, CuO powder have three peaks of the consumption of H_2 at ca. 295, 363 and 492 °C, respectively. With increase of Ce component, the peak at ca. 295 °C disappears. The peak at ca. 363 °C shift to the lower temperature and the consumption of H_2 become the less. The peak at ca. 492 °C shift to the lower temperature and the consumption of H_2 become rapidly less. CeO_2 powder have two peaks of the consumption of H_2 at ca. 520 °C and 892 °C. It is shown that the amounts of Ce component influence upon oxidation properties of the $\text{Ce}_{1-x}\text{Cu}_x\text{O}_{2-x}$ solid solution and there are

the synergistic reaction between the copper and ceria in the $\text{Ce}_{1-x}\text{Cu}_x\text{O}_{2-x}$ solid solution [13,14]. In the $\text{Ce}_{1-x}\text{Cu}_x\text{O}_{2-x}/\text{Al}_2\text{O}_3$ samples, $\text{CuO}/\text{Al}_2\text{O}_3$ have three peaks of the consumption of H_2 at ca. 188 °C, 292 °C and 746 °C, respectively. With increase of Ce component, the peak at ca. 188 °C disappears. The peak at ca. 292 °C shift to the higher temperature and the consumption of H_2 become the less. The peak at ca. 746 °C shift to the less temperature at the more Ce component and the consumption of H_2 become bigger. $\text{CeO}_2/\text{Al}_2\text{O}_3$ have three peaks of the consumption of H_2 at ca. 506, 538 and 690 °C, respectively. It is shown that both the Ce component of the $\text{Ce}_{1-x}\text{Cu}_x\text{O}_{2-x}$ solid solution and Al_2O_3 influence upon oxidation properties of the $\text{Ce}_{1-x}\text{Cu}_x\text{O}_{2-x}$.

Based on the above the H_2 -TPR results of the $\text{Ce}_{1-x}\text{Cu}_x\text{O}_{2-x}/\text{Al}_2\text{O}_3/\text{FeCrAl}$, the $\text{Ce}_{1-x}\text{Cu}_x\text{O}_{2-x}$ and the $\text{Ce}_{1-x}\text{Cu}_x\text{O}_{2-x}/\text{Al}_2\text{O}_3$, suggesting that there are the stronger interaction among the $\text{Ce}_{1-x}\text{Cu}_x\text{O}_{2-x}$ solid solution and the Al_2O_3 washcoats and the FeCrAl support. These change the redox performance of the samples and affect the catalytic activity of the catalysts.

4. Conclusions

$\text{Ce}_{1-x}\text{Cu}_x\text{O}_{2-x}$ ($x = 0-1$) solid solution based monolithic catalysts on supports FeCrAl alloy foils, with Al_2O_3 washcoats, were active for the catalytic combustion of methane. The particle shape and size of the $\text{Ce}_{1-x}\text{Cu}_x\text{O}_{2-x}$ solid solution and the catalytic performance of the catalysts depended on the ratio of the Ce and Cu in the $\text{Ce}_{1-x}\text{Cu}_x\text{O}_{2-x}$. The H_2 -TPR properties of the $\text{Ce}_{1-x}\text{Cu}_x\text{O}_{2-x}$, the $\text{Ce}_{1-x}\text{Cu}_x\text{O}_{2-x}/\text{Al}_2\text{O}_3$ and the $\text{Ce}_{1-x}\text{Cu}_x\text{O}_{2-x}/\text{Al}_2\text{O}_3/\text{FeCrAl}$ shown that there were the stronger interaction among the $\text{Ce}_{1-x}\text{Cu}_x\text{O}_{2-x}$ solid solution and the Al_2O_3 washcoats and the FeCrAl support.

Acknowledgements

Financial funds from the Chinese Natural Science Foundation (Project No.: 20136010, 20376005), Specialized Research Fund for the Doctoral Program of Higher Education (Project No.: 20030010002), SINOPEC and BUCT Young Teacher Research Fund (Project No.: QN0301) are gratefully acknowledged.

References

- [1] P. Gelin, M. Primet, Appl. Catal. B: Environ. 39 (2002) 1–37.
- [2] T.V. Choudhary, S. Banerjee, V.R. Choudhary, Appl. Catal. A: Gen. 234 (2002) 1–23.
- [3] M.V. Twigg, D.E. Webster, in: A. Cybulski, J.A. Moulijn (Eds.), Structured Catalysts and Reactors, Marcel Dekker, New York, 1998, pp. 59–90.

- [4] S. Roy, A.K. Heibel, W. Liu, T. Boger, *Chem. Eng. Sci.* 59 (2004) 957–966.
- [5] G. Groppi, W. Ibashi, E. Tronconi, P. Forzatti, *Chem. Eng. J.* 82 (2001) 57–71.
- [6] B. Kucharczyk, W. Tylus, L. Kepinski, *Appl. Catal. B: Environ.* 49 (2004) 27–37.
- [7] P. Artizzu, E. Garbowski, M. Primet, Y. Brulle, J. Saint-Just, *Catal. Today* 47 (1999) 83–93.
- [8] W. Liu, M. Flytzani-Stephanopoulos, *J. Catal.* 153 (1995) 317–332.
- [9] S. Ji, C. Li, Z. Lei, B. Chen, Patent Application Publication, CN 200310117394 (2003).
- [10] X. Wu, D. Weng, S. Zhao, W. Chen, *Surf. Coat. Technol.* 190 (2005) 434–439.
- [11] S. Zhao, J. Zhang, D. Weng, X. Wu, *Surf. Coat. Technol.* 167 (2003) 97–105.
- [12] P.J. Gellings, H.J.M. Bouwmeester, *Catal. Today* 58 (2000) 1–53.
- [13] G. Avgouropoulos, T. Ioannides, H. Matralis, *Appl. Catal. B: Environ.* 56 (2005) 87–93.
- [14] J.B. Wang, D.H. Tsai, T.J. Huang, *J. Catal.* 208 (2002) 370–380.